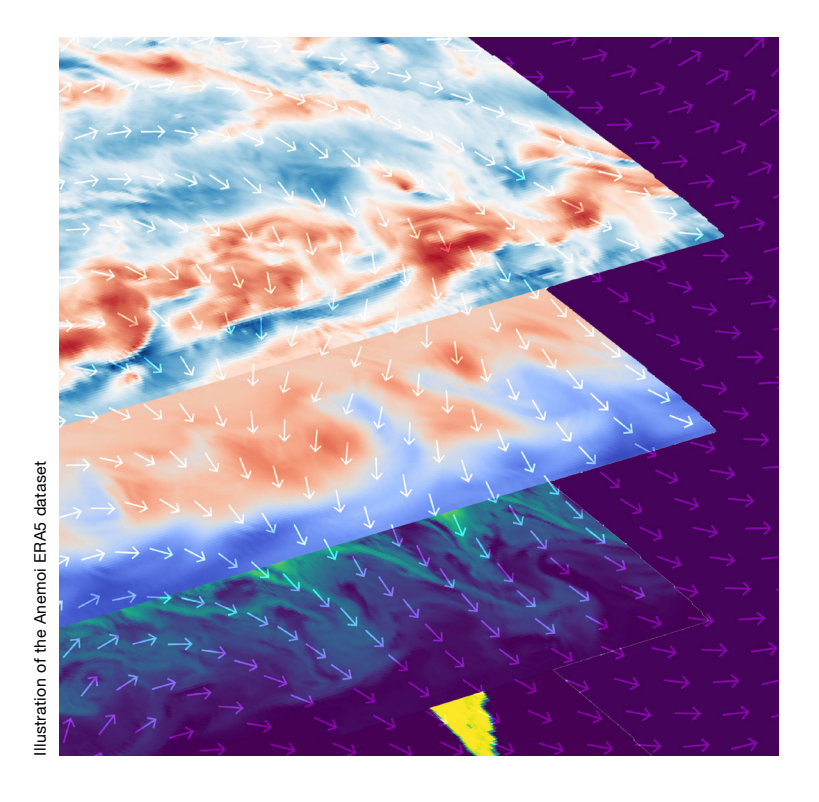


from Newsletter Number 185 - Autumn 2025

**EARTH SYSTEM SCIENCE** 

Upgrade to IFS Cycle 50r1



This article appeared in the Earth system science section of ECMWF Newsletter No. 185 – Autumn 2025, pp. 25–33

# **Upgrade to IFS Cycle 50r1**

## Inna Polichtchouk, Sébastien Massart, Zak Kipling

An upgrade to ECMWF's Integrated Forecasting System (IFS) is scheduled for operational implementation in early 2026. IFS Cycle 50r1 introduces a new ocean and sea ice configuration based on the NEMO4-SI<sup>3</sup> model (a state-of-the-art modelling framework used for research activities and forecasting services in ocean and climate sciences - Nucleus for European Modelling of the Ocean coupled with the Sea Ice Modelling Integrated Initiative is developed by a European consortium), alongside a new ocean data assimilation system. The level of ocean-atmosphere coupling in the four-dimensional variational (4D-Var) data assimilation system is enhanced by using outer-loop coupling, a method that increases the consistency of the ocean and atmospheric initial conditions. An additional 12-hour window ocean analysis is now running in parallel to the atmospheric analysis. Together, these changes improve the representation of ocean-sea ice-atmosphere interactions. The cycle also revises the treatment of convection with the aim of improving aspects such as inland propagation of convective precipitation. In the stratosphere, reduced vertical diffusion (small-scale mixing of air between different heights) improves representation of the quasi-biennial oscillation (QBO) of tropical zonal winds between easterly and westerly and of the humidity. The data assimilation will also be able to extract stratospheric humidity information from observations and make use of more 2-metre temperature observations. Cycle upgrades to the ensemble system include scale-selective re-centring in the Ensemble of Data Assimilations (EDA) and a revised Stochastically Perturbed Parametrizations (SPP) scheme, which represents model uncertainty, to reduce excessive 10-metre wind spread. Additional improvements include a new glacier scheme and refined wave-sea ice coupling. These developments result in more realistic coupled forecasts, better use of observations, through both assimilating more data and extracting more information from them, and reduced computational cost.

#### Key changes to the forecast model

IFS Cycle 50r1 introduces a wide range of improvements to the forecast model, targeting improved physical realism in convection, ocean and sea ice processes, land-surface interactions and stratospheric dynamics. It also addresses known forecast issues, such as stationary precipitation, excessive ensemble spread for surface winds and degraded tropical temperature biases.

A key change is a revision of how the model handles deep convection and cloud microphysics. A significant portion of convective precipitation is now handed over to the cloud scheme, where it is subject

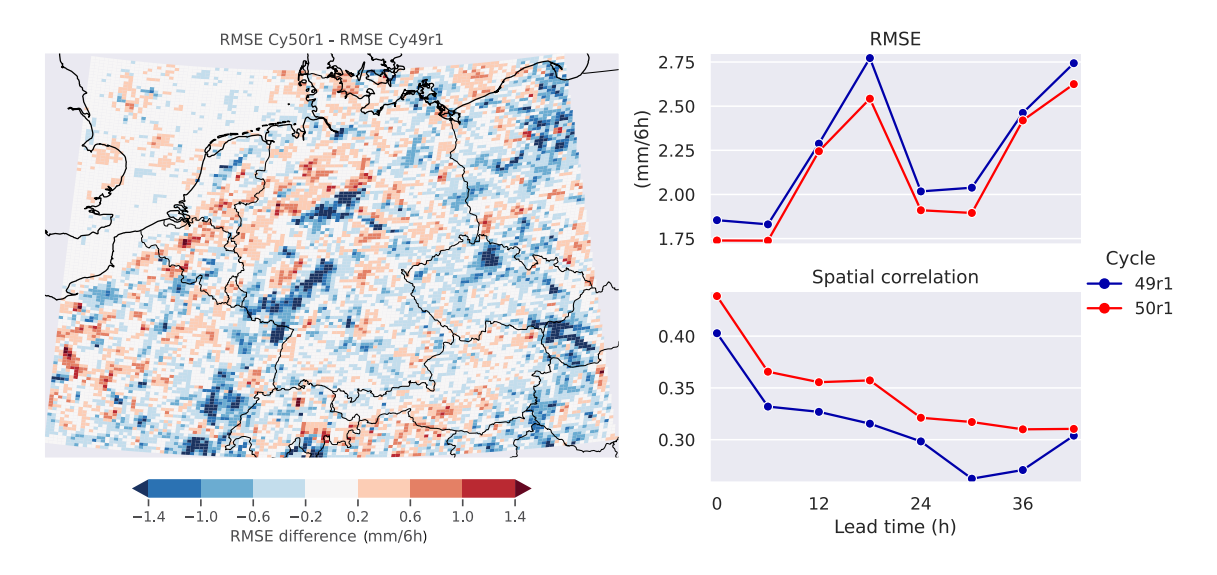


**FIGURE 1** Verification of rainfall forecasts against radar observations over Europe. The map shows the differences between Cycle 50r1 and Cycle 49r1 of root mean square error (RMSE) for all forecast lead times combined (blue indicates that 50r1 is improved), while the line plots show RMSE and spatial correlation as a function of lead time, averaged over Europe. Red lines correspond to Cycle 50r1 and blue lines to 49r1. Lower RMSE and higher correlation indicate improved forecast skill. Verification is performed for June 2024. Credit: Llorenc Lledó.

to advection and evaporation. This addresses the long-standing issue in the IFS of stationary convective precipitation, improving the representation of how precipitation propagates inland from the coast. Verification against radar observations shows that forecasts for precipitation over Europe and the USA have improved (see Figure 1).

The Stochastically Perturbed Parametrizations (SPP) scheme has been revised to address indications of excessive near-surface windspeeds in the ensemble (ENS). The SPP perturbations to surface momentum fluxes have been reduced by using a narrower range of random numbers and applying them with a uniform rather than log-normal transformation. These changes reduce the ensemble spread (the variance across ensemble members) in 10-metre wind speeds, especially over oceans, while maintaining ensemble reliability.

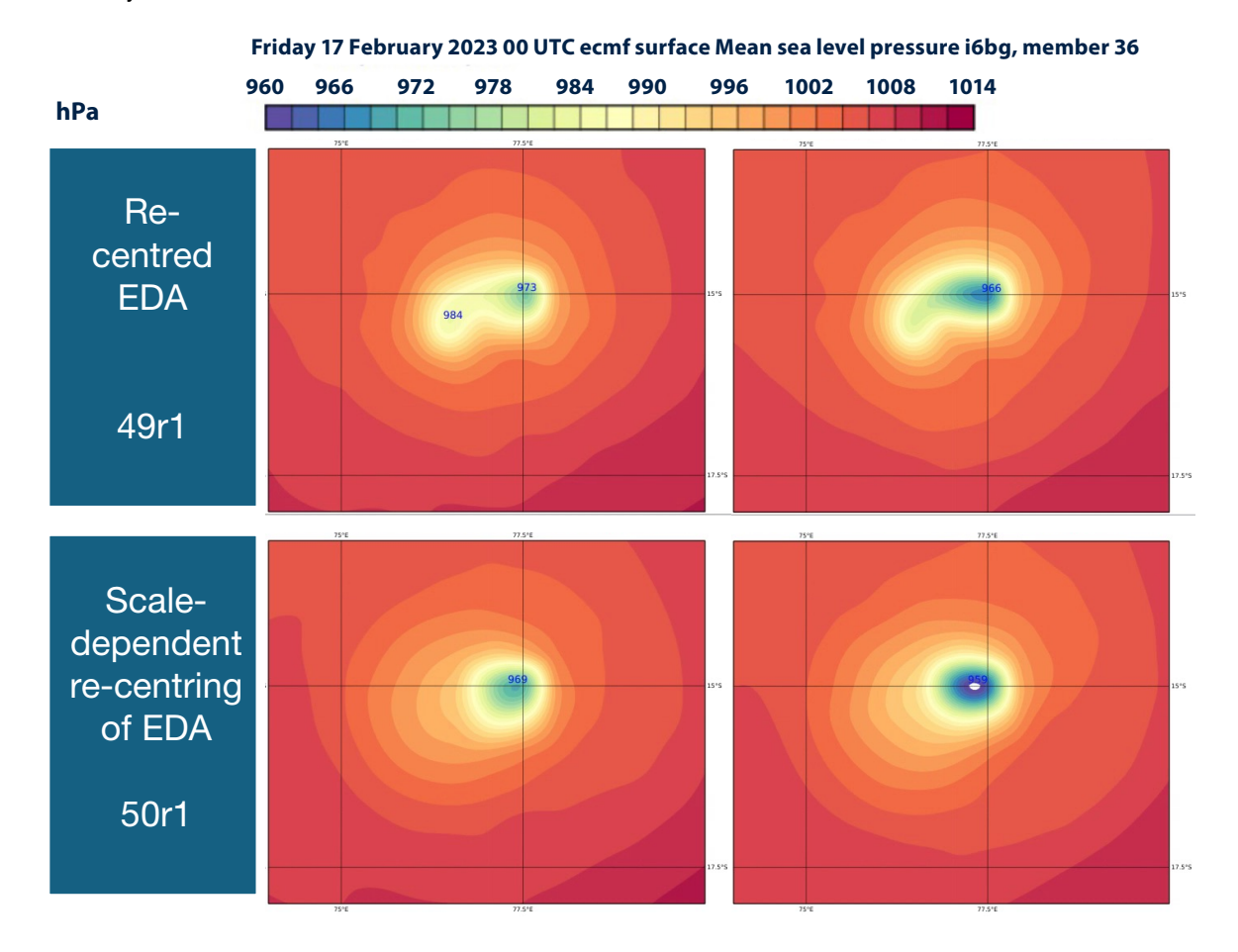


**FIGURE 2** Mean sea level pressure at forecast step = 0 h for Tropical Cyclone Freddy on 17 February 2023 at 00 UTC, shown for ENS members 36 and 45. The top panels show results with the old EDA re-centring (Cycle 49r1), while the bottom panels use the new scale-selective EDA re-centring to be introduced in Cycle 50r1. The new method removes the unrealistic 'double centre' feature present in the previous configuration. Credit: Sarah-Jane Lock and Martin Leutbecher.

To improve the realism of initial conditions in the ENS, particularly for tropical cyclones, a new method called scale-selective re-centring has been introduced in the EDA. Re-centring is now only applied to large-scale upper-air fields, centring them on the control forecast, while small-scale structures come directly from the EDA. This helps avoid unrealistic 'double-centred' tropical cyclones from appearing at the start of the ENS forecasts (see Figure 2).

The operational ocean system has been upgraded to NEMO4–Sl³, replacing the NEMO 3.4 + LIM2 configuration, introducing a multicategory sea ice model with prognostic salinity and meltpond dynamics, and an improved representation of the upper surface layers of the ocean. Partial coupling is switched off to enable fully coupled ocean–atmosphere forecasts, meaning the atmosphere now uses sea surface temperatures (SSTs) directly from the ocean model, replacing the previous approach – used outside

the tropics – where analysed SSTs were combined with ocean model tendencies The upgrade includes the coupling of snow depth and sea ice thickness from the sea ice model to the atmosphere, to allow snow over sea ice and variable ice thickness to be represented in the atmospheric forecast model. The improvements in sea ice concentration, upper-ocean mixing, SST diurnal cycle and thermodynamic consistency significantly reduce long-standing biases and enhance the realism and variability of ocean forecasts, while also halving the computational cost via single-precision arithmetic (Keeley et al., 2024).

The ocean wave model includes important scientific changes to its interaction with sea ice. Waves are now attenuated within the ice using the Sl<sup>3</sup> model when sea ice concentrations are above 30%, rather than being completely blocked, improving realism near the ice edges (Kousal et al., 2025).

On land, a new glacier scheme replaces the previous binary glacier mask with one that accounts for how much of the grid area is covered by ice and uses a four-layer land-ice scheme. This enables more accurate representation of snow and surface energy processes over fully and partially glaciated grid points, particularly in high-latitude and mountainous regions such as Greenland (Arduini et al., 2025).

In the stratosphere, vertical diffusion has been reduced under stable conditions, and the parametrized non-orographic gravity wave drag – representing the effect of atmospheric waves (not linked to mountains) that transport momentum and influence stratospheric winds – has been revised. This improves the representation of the QBO in the analysis and in forecasts on all time scales. In 50r1, QBO has a stronger amplitude and more realistic vertical descent (see Figure 3). Reduced vertical diffusion also helps to limit excessive moisture leakage from the troposphere into the stratosphere in the analysis and forecasts.

## Other updates include:

- · Revised aerosol climatology for radiation, which helps to improve tropical tropospheric temperatures.
- Reordering of physics, with vertical diffusion now applied last, improving near-surface 10-metre winds over the ocean.
- · Revised wave model bathymetry, improving surface wave realism.
- Use of surface currents in the wave model to account for refraction, resulting in reduced smoothing of wave fields.
- For calculating trajectories and in the minimisation, a small amount of off-centring was introduced in the semi-Lagrangian time-stepping method. This change noticeably improves how well the model fits stratospheric observations and leads to a modest improvement in stratospheric forecast skill.

#### Data assimilation and observation usage

IFS Cycle 50r1 introduces a significant step towards a more coupled data assimilation system, with an

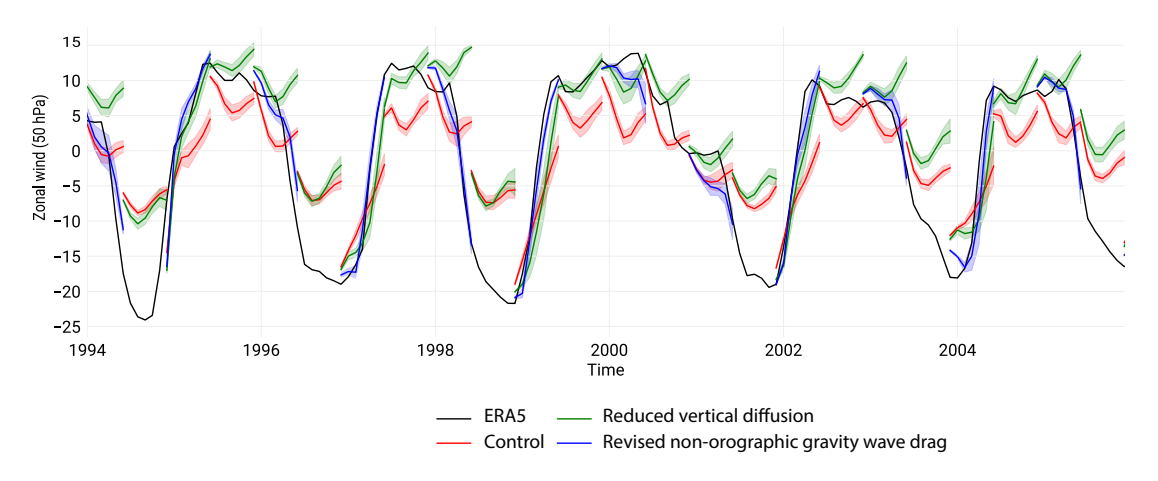
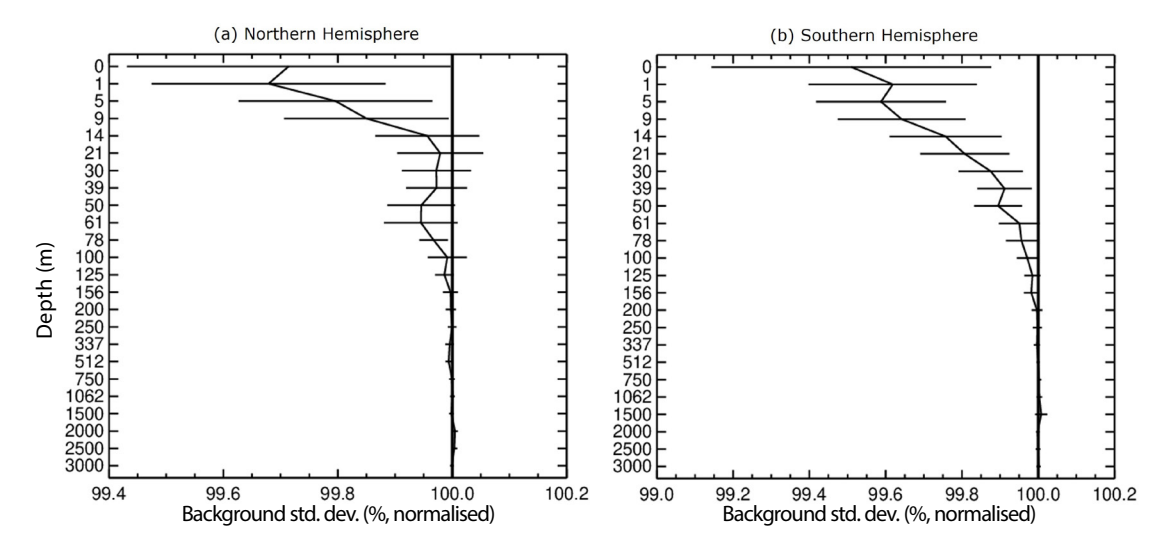


**FIGURE 3** Time series of zonal-mean zonal wind at 50 hPa, averaged over the equatorial belt (5°N–5°S), showing the quasibiennial oscillation in ERA5 reanalysis and in subseasonal-to-seasonal ensemble forecasts. The red line shows forecasts without reduced vertical diffusion; the green line includes reduced vertical diffusion in stable conditions; and the blue line includes both reduced vertical diffusion and the revised non-orographic gravity wave drag formulation to be introduced in Cycle 50r1. The revised configuration (blue) shows much better agreement with the reanalysis (ERA5). Credit: Annelize van Niekerk.

implementation of an outer-loop coupling type framework similar to that used in CERA reanalyses (Laloyaux et al., 2018) and building on the RADSST prototype (McNally et al., 2022).

First, the trajectories used to compare the model with observations are coupled between the atmosphere and ocean, allowing for more consistent representation of air-sea interactions during the assimilation window – the period over which observations are used to update the model's state.



—— = with observations of the ocean from MW imagers 100% = without observations of the ocean from MW imagers

**FIGURE 4** Relative change in the standard deviation of the background departures from ARGO floats when observations of ocean temperature from the microwave imagers are included in the coupled system. For (a) the Northern Hemisphere above 20°N and (b) the Southern Hemisphere (below 20°S) for the period 7 June 2022 to 31 August 2022 and 7 December 2022 to 28 February 2023 for the 00 UTC cycles. Credit: Tracy Scanlon.

Second, three-dimensional (3D) ocean and sea ice increments are computed in parallel to the 3D atmospheric increments. Although the ocean and atmosphere are adjusted separately, the system now makes a better use of select instruments with strong surface sensitivities. In this way, Level 1 data from low Earth orbit microwave instruments and geostationary infrared instruments are for the first time providing a constraint to the ocean and sea ice. This improves consistency between the coupled components and improves the accuracy of each (see Figure 4).

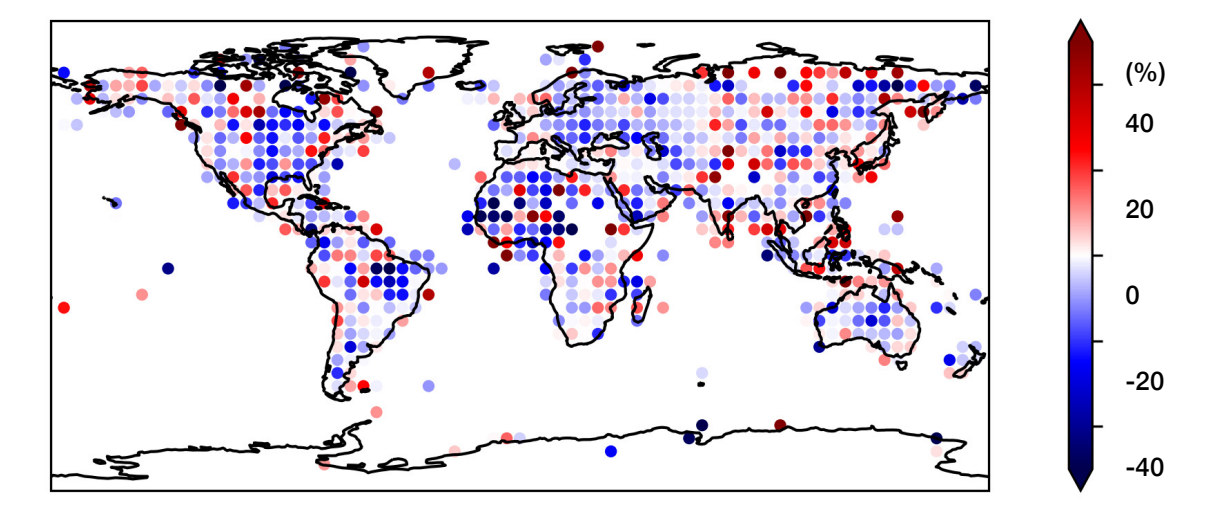


**FIGURE 5** Change in root mean square (RMS) first-guess departure (in %) for 2-metre temperature for IFS Cycle 50r1 when compared to observations assimilated in IFS Cycle 49r1. Statistics have been computed over July and August 2024, blue (red) means a reduction (increase) in RMS for IFS Cycle 50r1. Credit: Patrick Laloyaux.

			ccaf/seeps	rmsef/sdef	ccaf/seeps	rmsef/sdef	ccaf/seeps	rmsef/sdef
an	z	50	<b>VAAAAA</b>	******	***	A ***		
		100	ΔΔΔΔ	<b>▼</b> ∇∆∆∆	***	AA		
		250	<b>***</b>	****	<b>**</b>	<b>**</b>		
		500	▼ ΔΔ	▼ ▲▲▲△△△	<b>**</b>	<b>**</b>		
		850	Δ	Δ	***	<b>**</b>		
	msl		▼▼ ∆	▽	***	***		
	t	50	<b>**</b>	****	***	***	****	****
		100		ΔΑΑΑΔ	A & & & A & A & A & A & A & A & A & A &	ΔΔΔΔ	****	***
		250	<u> </u>	▽▼▼▼▼▼▼	<b>▲▲▲</b> ∇∇ <b>▼</b> ∇	<b>▲▲</b> ▽ <b>▼▼▼▼▼</b>	****	***
		500	ΔΑΑΑΔΔΔ	***	***	***	***	<b>A</b>
		850	<b>**</b>	****	***	****	***	***
	2t		***	<b>▲</b> △ <b>▼</b> ▽▽	***	AAAA	****	******
	vw	50	AAA 🗸	<b>▲ ****</b> ▽	AAAA	AAAA	****	***
		100	****	<b>▼▼▼</b> ▽	****	****▽	***	<b>▽</b> ▼▼▼▼▼▼▼▼
		250		<b>AAAA</b> A A A A	<b>▲▲▲</b> ▲△ ▽	<b>▲▲▲</b> △△ ♥♥♥	<b>AAA</b> A AAA	***
		500		****	AAAAA	AAAAA	<b>AAAAAA</b> AA	****
		850			AAAA	AAAAA	<b>AAA</b> A	
	10ff		ΔΔΔΔΔ ΔΔ	*******		****	<b>▲▽▼▼▼▼</b> ▽▽	
	r	250	<b>▼</b> △ △ △	******	AAAA	******	<b>VAA</b>	*******
	•	700	VAAAA		***	<b>*****</b>	<b>▼▼▼</b> Δ <b>Δ</b> Δ	<b>VV AAAAA</b>
	10ff@sea	700	<b>Δ</b> Δ <b>Δ</b> Δ ΔΔ	******	<b>***</b>	AAAAAAAA	***********	ΔΔ ∇
	swh			*****	****	*******	AAA	<u>ΑΔΑ</u> ΔΔΔΔ
	mwp		*****	*********	*****	********	AAAAAA	
ob	z	50	**	<b>*****</b>	AA		*****	*********
-	-	100	A AAA		Δ			
		250	▼ ΔΔ Δ	∇ ΔΔ ΔΔ Δ	Δ	A A		
		500	▼ ∆∆ ∆	** AA AAAA	∇	Δ Δ		
		850	ΔΔΔ ΔΔ	<b>ΔΔ</b> Δ Δ Δ	AAA	AAA		
	t	50	AAA AA	AAAAAAA	Δ	ΔΔΔΔΔΔ	***	****
	·	100		*****	Δ	ΔΔΔΔΔΔ		
		250	<b>AAA</b> Δ	<b>▲</b> ∇ <b>▼</b> ∇∇∇ <b>▼</b> ∇				****
		500	<b>▲</b> Δ		<b>▲</b> ΔΔ ∇	<b>▲▲</b> ▼∇∇		
			∇ ΔΔΔΔ Δ		ΔΔΔ	ΔΔΔ	Δ ΔΔ	Δ
		850	AA .	<b>AA</b>	Δ	ΔΔ Δ	<b>▽▼ ▼</b> ▽▽	** *
	2t			AA		▼ ΔΔΔ		******
	vw	50	<b>**</b>	AAA	***	***	****	****
		100	<b>▲</b> Δ	<b>A</b>	<b>AAA</b> Δ	<b>**</b>	<b>A A A A A A A A</b>	∇
		250	Δ 🛦 Δ Δ	ΔΔΔΔ	Δ Δ Δ ∇	$\nabla$ $\Delta$ $\nabla\nabla$	Δ	
		500		****	ΔΔΔΔ ∇	ΔΔΔΔ	Δ	ΔΔ Δ Δ Δ
		850	ΔΔΔ Δ Δ	ΔΔ▲ Δ ▲	Δ ∇			Δ
	10ff			△▲▲		▼▽▽△		****
	r	250	Δ	******		****		******
		700	✓	<b>■ ▲ △ ▲ ▲ ▲ △ ▲</b>	Δ Δ		▼▽	▼▽ ▲▲
	2d			****		****		****
	tcc			****		****		****
	tp		Δ ΔΔΔ	****	ΔΔ Δ	A	Δ	<b>**</b>
	swh							

ccaf=Anomaly correlation,maef=Mean absolute error,rmsef=Root mean square error,sdaf=Standard deviation of forecast anomaly,sdef=Standard deviation of forecast error,seeps=Stable Equitable Error in Probability Space

Each error plot is converted into a sequence of symbols (e.g. ▼▼

△▲) where each symbol indicates for given time step whether the experiment is significantly better or worse than the control on different confidence levels.

Symbol legend: for a given forecast step...

▲ experiment better than control statistically significant with 99.7%

- $\triangle$  experiment **better** than control statistically **significant with 95% confidence**
- experiment better than control statistically **significant with 50% confidence**
- not really any difference between control and experiment
- experiment worse than control statistically **significant with 50% confidence**
- ▼experiment worse than control statistically significant with 95% confidence
- ▼ experiment worse than control statistically significant with 99.7% confidence

**FIGURE 6** Summary scorecard comparing the difference between control forecasts from IFS Cycle 50r1 and IFS Cycle 49r1 using anomaly correlation coefficients and the root mean square error (RMSE). Note that total precipitation is evaluated using the Stable Equitable Error in Probability Space (SEEPS) score rather than correlation, and wave parameters are evaluated using the standard deviation of errors rather than RMSE. Blue symbols and shading indicate improvements in IFS Cycle 50r1 with respect to IFS Cycle 49r1. Red symbols and shading indicate degradation. Scores are calculated from over 420 forecasts initialised at 00 and 12 UTC between 1 May 2024 and 14 July 2025.

			n.h	em	s.he	em	tropics		
			ccaf/seeps	crps	ccaf/seeps	crps	ccaf/seeps	crps	
ın	z	50	****	Δ ************************************	<b>***</b>	<b>▲</b> △ ▽ <b>▼▼▼▼▼▼</b> ▼▼			
		100	<b>***</b>	***	<b>***</b>	<b>**</b>			
		250	**	<b>***</b>	<b>**</b>	<b>***</b>			
		500	<b>▼</b> ▽	▼ Δ	<b>**</b>	<b>***</b>			
		850	Δ∇∇	<b>△</b> ∇∇ ∇	<b>AAA</b>	***			
	msl		¥₹∇∇	V▼V	<b>**</b>	****			
	t	50	<b>**</b>	****	****	****	****	****	
		100	****	Δ	<b>***</b>	<b>▲</b>	****	*****	
		250		▽▽▼▼▼▼▼	***		*****	*****	
		500	<b>▼▼</b> ▽	ΔΑΑΑΑΑΔ ΔΔ	<b>A</b> AAA	*****	<b>▲▲▲</b> △	<b>A</b>	
		850	ΔΔΔ	ΔΔΔ ΔΔ	****	ΔΔΔΔΔΔ Δ	**************************************	*****	
	ff	50	ΔΔΔΔΔ	<b>▲▲▲</b> △ 🗆 🗸	*****	****	****	*****	
		100	$\nabla$	<b>▼▼▼▼▼▼</b> ▽▽▽▽	<b>▽▼</b>	ΔΔ	Δ.Δ.	<b>₩</b>	
		250		▼ ▽	<b>**</b>	<b>▲▲▲</b> △	<b>▲</b> △△ △△ △ △	<b>▲</b> ▽	
		500			****	<b>**</b>	*****	****	
		850	Δ	Δ	<b>**</b>	<b>A</b>	<b>**</b>	<b>▲▲</b> ░▽▽▼▼▼▼	
	r	250	****	***********		******	Δ	******	
		700	▼	▼	****	****	∇ <b>▼</b> ∇∇	******	
	2t			∆∆∆∭∇∇ <b>▼</b> ∇∇ <b>▼</b> ∇∇	ΔΔΔΔΔ	∇ Δ	****	<b>▲▲</b> △	
	10ff@ sea		***	*****	***	*****	****	*****	
	swh		*****	*****	*****	*****	*****	*****	
_	mwp		*****	************	****	***********	****	*****	
b	z	50	<b>▼▼</b> ▽▼▼ ΔΔΔΔ	<b>*</b> ***********		VAA *********			
		100	<b>**</b>	▲△		▼ Δ ΔΔ			
		250		<b>A</b>	Δ <b>Δ</b> Δ <b>Δ</b>	ΔΔΔ ΔΔΔ			
		500	$\nabla\nabla$	***	<b>▼</b> ▽ ΔΔ	Δ			
		850		<b>▲▲</b>	ΔΔ Δ	Δ ΔΔΔ Δ Δ			
	t	50	<b>***</b>	****	<b>A</b> AA AA A	*****	*****	*****	
		100		<b>AA</b>	ΔΑΑΑΑΑ	<b>▲▲▲▲▲</b>	*****		
		250	<b>▲</b> △ <b>▼</b> ▽		<b>AA</b> Δ Δ Δ Δ		<b>***</b>	*****	
		500	<b>▼▼</b> ▽	▼▼▽	Δ Δ	Δ Δ		<b>▽**********</b>	
		850	<b>▲▲</b>	A	ΔΔΔΔ	Δ	$\nabla\nabla$	∇ ΔΔΔΔΔΔΔΔΔΔΔΔ	
	ff	50	<b>***</b>	***	<b>***</b>	****	****	*****	
		100	***	***	****	*****	ΔΔΔΔ	<b>▲</b> ΔΔ Δ	
		250		<b>▲</b> △	Δ	A	Δ ***	****▽	
		500		▼▼ ∇∇	Δ	Δ	∇		
		850		<b>▽</b>	Δ ΔΔ	ΔΔΔ			
	r	250	▽	******	▽	*****		<b>******</b>	
		700	∇ Δ Δ ΔΔ	Δ	ΔΔΑ Δ ΔΑΔ	Δ Δ Δ Δ Δ Δ		∇	
	2t			<b>**</b>		<b>▼▼</b> ▽			
	2d					ΔΔΔΔ Δ		****	
	tcc			****		*****		*****	
	10ff			******		***************************************		***********	
						******			
	tp			******		***************************************		***********	

ccaf=Anomaly correlation,maef=Mean absolute error,rmsef=Root mean square error,sdaf=Standard deviation of forecast anomaly,sdef=Standard deviation of forecast error,seeps=Stable Equitable Error in Probability Space

Each error plot is converted into a sequence of symbols (e.g. ▼▼

△▲) where each symbol indicates for given time step whether the experiment is significantly better or worse than the control on different confidence levels.

Symbol legend: for a given forecast step...

experiment better than control statistically significant with 99.7% confidence

- $\triangle$  experiment  ${\bf better}$  than control statistically  ${\bf significant}$  with  ${\bf 95\%}$  confidence
- experiment better than control statistically **significant with 50% confidence**
- not really any difference between control and experiment
- experiment worse than control statistically significant with 50% confidence
- ▼ experiment worse than control statistically significant with 95% confidence
- ▼ experiment worse than control statistically significant with 99.7% confidence

**FIGURE 7** Summary scorecard comparing the difference between ensemble forecasts with IFS Cycle 50r1 and IFS Cycle 49r1, using the anomaly correlation coefficient (ACC) of the ensemble mean and the continuous ranked probability score (CRPS). Blue symbols and shading indicate improvements in IFS Cycle 50r1 with respect to IFS Cycle 49r1. Red symbols and shading indicate degradation. Scores are calculated using 50 perturbed ensemble members from more than 117 forecasts initialised at 00 UTC between 1 June 2024 and 21 June 2025.

Ocean and sea ice initial conditions for these coupled analyses still come from an ocean long-window analysis generated in a weakly coupled manner and referred to as outer-loop coupled data assimilation (OLDA). For the first time, this ocean analysis is based on the same IFS cycle as other streams and will be available in ECMWF's Meteorological Archival and Retrieval System (MARS) (under stream OLDA). Its initial conditions are taken from the ORAS6 reanalysis, ensuring long-term consistency.

One of the key purposes of this cycle is to improve the computational efficiency of the IFS. A significant step is the implementation of single-precision computation in the coupled atmosphere—ocean trajectory – where the ocean and atmospheric models are run together and so remain consistent. Efficiency gains were also made in the EDA by running the first minimisation at a reduced horizontal resolution, from TL399 to TL255. Together, these adjustments reduce computational requirements by about 40%, while maintaining the quality of the ensemble background error estimates.

Another significant improvement of this cycle is the modification to the weak-constraint 4D-Var system, so that biases in the model are now evolving over the full 12-hour data assimilation window. To account for the diurnal variations in model error, the correction in 50r1 follows a first-order Fourier decomposition over time. This is implemented for the stratosphere, the boundary layer and the top soil temperature level. The result is significant improvements in the boundary layer, including a 3% reduction in the root mean square first-guess departure – the difference between the first trajectory of the new assimilation cycle and the observations – for 2-metre temperature (T2m) when compared to IFS Cycle 49r1 (see Figure 5). By reducing model biases in the boundary layer and therefore better constraining the model's atmospheric mean state, the system can now assimilate T2m observations over the full 12-hour window instead of just the first six hours.

The treatment of humidity in the upper troposphere and lower stratosphere (UTLS) has also been improved within the 4D-Var analysis. Previously, humidity increments in the stratosphere were artificially set to zero, limiting the ability of the system to adjust humidity fields here. Removal of this constraint has allowed the analysis to produce physically consistent humidity increments throughout the UTLS. In addition, the vertical coverage of radiosonde humidity observations has been extended up to 60 hPa. This provides improved observational constraints in the lower stratosphere, contributing to a more accurate and dynamically consistent representation of moisture in the UTLS (Semane and Bonavita, 2025).

#### Other updates include:

- Upgrading of the radiative transfer model to RTTOV-14.0, which improves the accuracy of radiance simulations.
- Upgrading the surface emissivity model over sea ice, so it can now be used up to 183 GHz compared to the previous upper limit of 89 GHz. This applies to all-sky microwave channels and would improve the analysis in polar regions under cloudy conditions.
- The spatial density of geostationary satellite data has been increased by reducing the minimum spacing used to select the data the thinning distance from 125 km to 75 km, and the time resolution has been improved by using hourly data. In parallel, window channels frequency bands where the atmosphere is relatively transparent have been included in the assimilation.
- Observations are now re-selected a process known as re-screening for every trajectory of the outer-loop framework to ensure consistent use of the best data, based on a better knowledge of the atmospheric state.
- The length of the observation timeslots has been reduced from 30 minutes to 15 minutes, allowing for a more accurate comparison between the model and the observations. The observations are clustered into 'timeslots' over the 12-hour assimilation window, with all the observations within a given timeslot assigned the same time (rather than their 'true' time).
- A different method has been introduced to compute the background error standard deviation from the EDA, giving a more realistic spread distribution between the extra-tropics and the tropics.
- Wind increments derived from ozone-sensitive observations in the lower and mid-stratosphere have been restored, avoiding regions where heterogeneous chemistry may occur.

## Impact on medium-range and sub-seasonal forecasts

Scorecards summarising forecast performance for the control forecast and the ENS are shown in Figure 6 and Figure 7, respectively. Both scorecards are predominantly blue, indicating that the new IFS Cycle 50r1 generally improves the forecast skill across a wide range of variables and lead times.

Improvements in both the control forecast and ENS include:

- Forecasts of QBO improved by up to 15%, due to reduced vertical diffusion and the revised nonorographic gravity wave drag formulation.
- Temperatures and winds at 850 and 250 hPa in the tropics improved by up to 7%, with contributions from the updated aerosol climatology, revised convection scheme and reordering of physics.
- Forecasts of total cloud cover, dewpoint temperature and 10-metre winds over sea improved by 1–2%, largely due to changes in the physics of the model.

Degradations in both the control forecast and ENS include:

- 250 hPa relative humidity evaluated using root mean square error (RMSE) and continuous ranked probability (CRPS) scores – degraded by around 2%.
- 50 hPa geopotential height (using RMSE and CRPS) degraded by up to 15%, mainly due to a shift in mean values associated with the revised aerosol climatology.
- Forecasts of 2-metre temperature in the tropics degraded by 1–2% (using RMSE and CRPS), due
  to a bias shift linked to changes in the physics of the model (including aerosol climatology update),
  resulting in slightly colder-than-observed temperatures over land.

Forecast accuracy for total precipitation and 10-metre winds has improved by 1–2% in both the control forecast and the ensemble mean, using RMSE (see also Figure 1 for radar-based rainfall verification). The Stable Equitable Error in Probability Space (SEEPS) score also shows improvement for total precipitation in the control forecast. However, when evaluated using CRPS, these variables show degradations of up to 3% in the ENS. These degradations in 10-metre winds can largely be explained by the revision of the SPP scheme, which significantly reduces ensemble spread (by 15% for 10-metre winds), addressing the spurious wind extremes and spread present in Cycle 49r1. However, when accounting for observation uncertainty in the form of representativeness errors (Bouallègue, 2020), verification shows that 10-metre wind CRPS scores are nearly comparable between Cycles 49r1 and 50r1, and the apparent degradation in total precipitation CRPS is halved (Figure 8).

The remaining degradation in total precipitation CRPS score in the ENS is attributed to physics changes in the model that result in a slight shift in the precipitation distribution. Cycle 50r1 produces approximately 1% more precipitation overall, with a small shift toward lighter rainfall amounts at the lower end.

Small improvements to tropical cyclone intensity and position forecasts have been observed in the control forecast. At the sub-seasonal time range (up to 46 days ahead), the most notable improvements come from the enhanced representation of the QBO, sea-surface temperatures and sea ice, with benefits that persist across all lead times.

## System configuration changes and updated products

IFS Cycle 50r1 does not introduce changes to the horizontal or vertical resolution. However, there will be several product updates. The high-resolution deterministic forecast (HRES) will be retired as a separate product and instead moved under the control forecast category in the MARS archive and in dissemination. In addition, ocean long window analysis data will also be made available in MARS.

#### Summary and outlook

IFS Cycle 50r1 brings major advances in both the forecast model and the data assimilation system, marking a significant step forward in coupled Earth system prediction. The model upgrade includes the introduction of the NEMO4-Sl<sup>3</sup> ocean and sea ice model, improved wave–ice interactions, revised vertical diffusion and gravity wave drag in the stratosphere, changes to the convection scheme, a new glacier scheme, and a revised SPP scheme that reduces excessive near-surface wind spread in the ensemble.

On the data assimilation side, a new atmosphere–ocean coupled analysis configuration enables assimilation of Level 1 satellite data into the ocean and sea ice, while weak-constraint 4D-Var introduces time-varying model errors and has been extended to the boundary layer.

Cost-efficiency improvements have been made through the use of single-precision trajectories, single-precision ocean model and from reducing the resolution of the first minimisation in the EDA. The system now allows humidity increments in the stratosphere, addressing longstanding issues in moisture analysis at these levels.

Together, these upgrades improve the representation of stratospheric dynamics, tropical upper-air structure, and the interactions between ocean, sea ice and the atmosphere, while reducing computational cost and laying the foundation for future advances in coupled data assimilation.

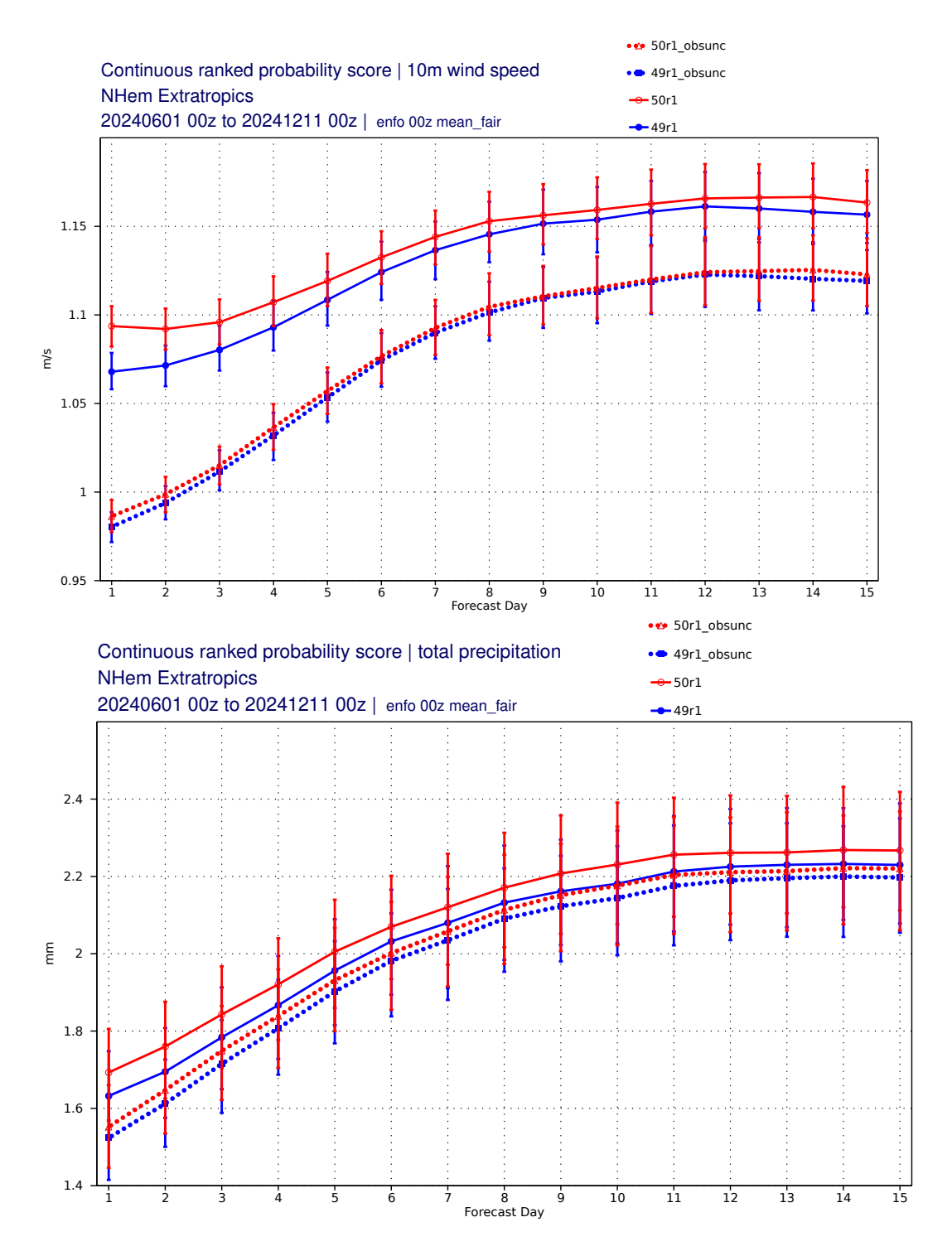


**FIGURE 8** Continuous ranked probability score (CRPS) for (top) 10-metre winds and (bottom) total precipitation from Cycle 49r1 (blue) and Cycle 50r1 (red), verified against observations and averaged over the Northern Hemisphere extratropics. The solid lines show CRPS without accounting for observation uncertainty and the dotted lines show CRPS when accounting for observation uncertainty. All scores are calculated using 50 perturbed members from 77 forecasts initialised daily between 1 June 2024 to 5 August 2024 and between 1 December 2024 and 11 December 2024.

## **Further reading**

Keeley, S., K. Mogensen, J-R. Bidlot, M. Balmaseda and S. Hatfield, 2024: Introduction of a new ocean and sea ice model based on NEMO4-SI3. ECMWF Newsletter No. 180, 24–29. https://doi.org/10.21957/sk4928ds0a

**Arduini, G., C. Rüdiger. and G. Balsamo,** 2025: An improved glacier parameterisation for the ecLand land-surface model: local, regional and global impact, EGUsphere [preprint], https://doi.org/10.5194/egusphere-2025-2454

Kousal, J., J. Bidlot, J. Rabault and M. Müller, 2025: The introduction of waves in sea ice. *ECMWF Newsletter* No. 185. 18–19

https://www.ecmwf.int/en/elibrary/81689-newsletter-no-185-autumn-2025

Laloyaux, P., E. de Boisseson, M. Balmaseda, J-R. Bidlot, S. Broennimann, R. Buizza, et al., 2018: CERA-20C: A coupled reanalysis of the twentieth century. J. Adv. Model. Earth Syst., 10, 1172–1195. https://doi.org/10.1029/2018MS001273

**Semane, N. and M. Bonavita,** 2025: Reintroducing the analysis of humidity in the stratosphere. *ECMWF Newsletter* **No. 183,** 28–31. https://doi.org/10.21957/ns41h80kl3

**Ben-Bouallègue, Z.** 2020: Accounting for representativeness in the verification of ensemble forecasts. ECMWF Tech. Memo. 865. <a href="https://doi.org/10.21957/5z6esc7wr">https://doi.org/10.21957/5z6esc7wr</a>

McNally, T., P. Browne, M. Chrust, D. Fairbairn, S. Massart, K. Mogensen and H. Zuo, 2022: Progress on developing a new coupled sea-surface temperature analysis. *ECMWF Newsletter* **No. 172**, 17–22. https://doi.org/10.21957/tm4913hs8d

#### **Acknowledgements**

We thank Llorenç Lledó, Annelize van Niekerk, Sarah-Jane Lock, Martin Leutbecher, Tracy Scanlon, Patrick Laloyaux, Philip Browne, Sarah Keeley, and Gabriele Arduini for providing figures and valuable input to this article.

## © Copyright 2025

European Centre for Medium-Range Weather Forecasts, Shinfield Park, Reading, RG2 9AX, UK

The content of this document, excluding images representing individuals, is available for use under a Creative Commons Attribution 4.0 International Public License. See the terms at <a href="https://creativecommons.org/licenses/by/4.0/">https://creativecommons.org/licenses/by/4.0/</a>. To request permission to use images representing individuals, please contact pressoffice@ecmwf.int.

The information within this publication is given in good faith and considered to be true, but ECMWF accepts no liability for error or omission or for loss or damage arising from its use.